Electrochemistry of Encapsulated Guests: Ferrocene inside Cram's Hemicarcerands

Sandra Mendoza, Pablo D. Davidov, and Angel E. Kaifer*

Abstract: The voltammetric behavior of ferrocene encapsulated inside two hemicarcerand hosts was investigated in dichloromethane and tetrachloroethane solutions. Molecular encapsulation led to substantial changes in the anodic voltammetric behavior of the ferrocene nucleus. Generally, encapsulated ferrocene exhibited a more positive half-wave oxidation potential and a lower apparent standard rate constant of heterogeneous electron transfer than uncomplexed ferrocene under identical experimental conditions. Whereas the anodic shift of the half-wave potential probably results from the hindered solvation of the positively charged, oxidized ferrocene inside the nonpolar hemicarcerand cavities, the observed decrease in electron transfer rate seems to arise primarily from the increased molecular mass of the electro-inactive species and the longer distance of maximum approach between the ferrocene center and the electrode surface which is imposed by the encapsulating host. Generally, electrochemical oxidation did not significantly alter the slow rate of ferrocene guest dissociation or release from the hemicarceplexes surveyed.

Keywords: electron transfer · ferrocenes · hemicarcerands · host–guest chemistry · molecular encapsulation · sandwich complexes · voltammetry

Introduction

Redox reactions are particularly important in chemistry and have therefore been the subject of extensive theoretical and experimental research work. Indeed, Marcus and others have provided detailed theoretical formulations which have successfully explained many experimental findings on the kinetics of electron transfer (ET) processes.[1–6] During the last decade, the development of supramolecular chemistry[7] has opened the possibility of investigating redox processes coupled to more complicated chemical events, such as inclusion complexation. A few years ago the electrochemical oxidation of ferrocenecarboxylic acid in the presence of β-cyclodextrin was studied in detail.[8] In aqueous solution this molecular receptor forms a stable inclusion complex with the ferrocene moiety, but according to Evans and co-workers the inclusion complex does not undergo direct oxidation at the electrode surface.[8] Instead, electron transfer from the ferrocene to the electrode takes place only after dissociation of the inclusion complex. We have shown similar behavior for the oxidation of a series of positively charged ferrocene derivatives in the presence of β-cyclodextrin[9] as well as, more recently, for the oxidation of fully reduced viologen derivatives[10] and cobaltocene,[11] which are also strongly complexed by β-cyclodextrin. All of these complexes are formed reversibly in solution; that is, the inclusion complexes are kinetically labile, with typical dissociation rate constants around $10^4\ s^{-1}$. Under these conditions, the heterogeneous ET process may circumvent the inclusion complex simply because the free guest is available on the experimental time scale. What would be the observed electron transfer behavior, however, if the inclusion complex were kinetically inert, that is, if the electro-inactive guest were constrained to remain encapsulated inside the host for a long time? In more general terms, the question would be: how does complete molecular encapsulation affect the electron transfer reactions of redox-active centers?

Intrigued by the findings on cyclodextrin inclusion complexes, we have started a research program geared to answering these questions. As a first step in our program, we recently reported the electrochemical behavior of benzidine (BZ) and *p*-phenylenediamine (PDA) when inserted as the central components of rotaxanes[12] (see Figure 1). Although the molecular architecture of these compounds does not afford perfect encapsulation, the anodic electrochemistry of the BZ and PDA subunits is profoundly affected by the continuous proximity of the tetracationic cyclophane which was used as the bead in these rotaxanes. In fact, the two consecutive monoelectronic oxidations of *p*-phenylenediamine were hindered both thermodynamically (the half-wave

[*] Prof. A. E. Kaifer, S. Mendoza, P. D. Davidov,
Chemistry Department, University of Miami
Coral Gables, FL 33124-0431 (USA)
Fax: (+49) 305 444-1777
E-mail: akaifer@umiami.ir.miami.edu

0947-6539/98/0405-0864 $ 17.50+.50/0

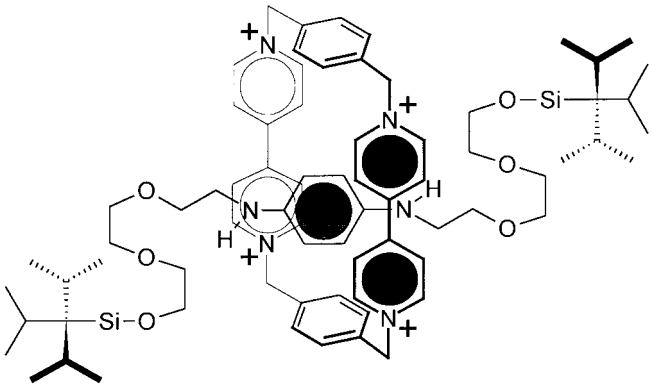

Figure 1. Structure of a rotaxane with a *p*-phenylenediamine core.

potentials were anodically shifted) and kinetically,[12] as evidenced by the observed decrease of the apparent standard rate constants (k^0) for the heterogeneous ET processes. Similar, although quantitatively smaller, effects were observed with the corresponding BZ rotaxane. Unquestionably, these effects may just be the result of the strong electrostatic interactions prevalent in these rotaxane structures, especially upon one- or two-electron oxidation of the core BZ or PDA subunits.

In order to encapsulate redox-active centers fully inside a neutral organic structure, we turned to Cram's hemicarcerands[13] (see structures **1** and **2**), a fascinating type of host that

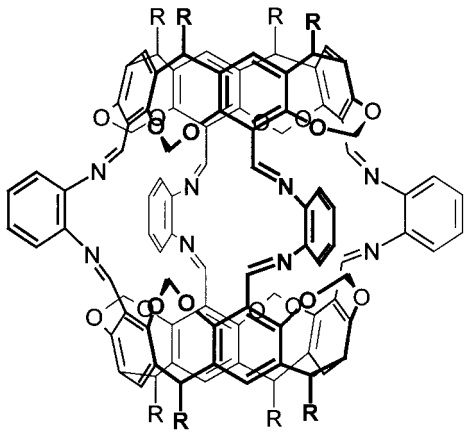

1, R = -CH_2CH_2Ph
2, R = -$(CH_2)_4CH_3$

can form inclusion complexes of high kinetic stability with molecular guests of moderate size, such as the redox-active ferrocene.[14] Guests of appropriate size and shape can access the hemicarcerand cavity through the four equatorial openings or portals defined by the four bridges joining the two cavitand halves of the host. However, the formation of the corresponding inclusion complexes, or hemicarceplexes, can be extremely slow at room temperature if the sizes of the guest and the portals are similar. The rate of association can be increased at higher temperatures; upon cooling, the guest becomes kinetically trapped inside the host cavity because the dissociation rate is also exceedingly slow. Cram has coined the term constrictive binding in reference to these host–guest phenomena[13] and proposed that the cavity of these hosts represents a new state of matter. In this regard, Cram and his co-workers have demonstrated that cyclobutadiene is stabilized inside these hosts,[15] proton-transfer equilibria are strongly affected by encapsulation,[16] and encapsulated guests can undergo chemical oxidation or reduction reactions.[17] Very recently, Balzani and co-workers[18, 19] as well as Farran et al.[20, 21] have investigated the photophysical properties of encapsulated guests. Here we report, for the first time, the electrochemical behavior of ferrocene encapsulated inside these intriguing molecular containers.

Experimental Section

Materials: Hemicarcerands **1** and **2** were synthesized following the general methodology described by Cram and co-workers.[13] The preparation of the tetrabromo cavitands is fully reported in the literature.[22, 23] The remaining compounds were prepared as follows.

Tetral cavitand with phenylethyl feet (**5**): A solution of tetrabromide **3** (2.5 g, 2.05 mmol) in THF (175 mL) was maintained under a dry nitrogen atmosphere at −78 °C and *sec*-butyllithium (17.5 mL, 22.5 mmol) was added dropwise. The mixture was stirred for 20 min after the addition was completed and then *N*-formylmorpholine (1.75 mL, 22.5 mmol) was added. After the solution had been allowed to warm slowly to 25 °C, 3 N HCl was added until the solution became acidic. The solvent was evaporated under vacuum, then the residue was filtered and washed with water. The crude solid was chromatographed on silica gel with CH_2Cl_2/AcOEt (95:5 v/v; $R_f = 0.27$). The tetraaldehyde was isolated as a white crystalline solid (370 mg, 16 %). ^{1}H NMR (400 MHz, $CDCl_3$): $\delta = 2.4-2.68$ (m, 16H), 4.47 (d, $J = 7.3$ Hz, 4H), 4.98 (t, $J = 8$ Hz, 4H), 5.89 (d, $J = 7.3$ Hz, 4H), 7.11–7.22 (m, 20H), 7.29 (s, 4H), 10.25 (s, 4H).

Tetral cavitand with pentyl feet (**6**): Starting from the tetrabromocavitand **4** (3.0 g, 2.6 mmol), the procedure was identical to that followed for the preparation of **5**. The product was obtained as a white crystalline solid (0. 41 g, 17 %). $R_f = 0.31$ (silica gel, CH_2Cl_2/AcOEt, 95:5 v/v); ^{1}H NMR (400 MHz, $CDCl_3$): $\delta = 0.93$ (t, $J = -7.2$ Hz, 12H), 1.38 (m, 24H), 2.23 (m, 8H), 4.47 (d, $J = 7.6$ Hz, 4H), 4.91 (t, $J = 8$ Hz, 4H), 5.89 (d, $J = 7.6$ Hz, 4H), 7.28 (s, 4H), 10.25 (s, 4H).

Hemicarcerand with phenylethyl feet (**1**): To a stirred solution of tetral cavitand **5** (634 mg, 0.595 mmol) in CH_2Cl_2 (100 mL) was added 1,3-diaminobenzene (130 mg, 1.2 mmol). A small amount (spatula) of magnesium sulfate was added and the reaction mixture was stirred for six days at room temperature under a nitrogen atmosphere. The resulting solution was filtered through celite, and the filtrate was evaporated. The crude product was chromatographed on silica gel (CH_2Cl_2/hexane, 70:30 v/v; $R_f = 0.40$) and crystallized from CH_2Cl_2/MeOH to provide **1** as a yellowish solid (265 mg, 39 %). ^{1}H NMR (400 MHz, $CDCl_3$): $\delta = 2.6-2.74$ (m, 16H), 4.69 (d, $J = 7.7$ Hz, 4H), 5.08 (t, $J = 8$ Hz, 4H), 5.73 (d, $J = 7.7$ Hz, 4H), 6.61 (s, 4H), 6.82 (d d, $J = 7.8$ and 2 Hz, 8H), 7.20–7.27 (m, 20H), 7.31 (s, 4H), 7.39 (t, $J = 8$ Hz, 4H), 8.49 (s, 8H).

Hemicarcerand with pentyl feet (**2**). To a stirred solution of tetral cavitand **6** (735 mg, 0.791 mmol) in CH_2Cl_2 (100 mL) was added 1,3-diaminobenzene (171.2 mg, 1.583 mmol). A spatula of magnesium sulfate was added and the reaction mixture was stirred for six days at room temperature under a nitrogen atmosphere. The resulting solution was filtered through celite, and the filtrate was evaporated. The crude product was chromatographed on silica gel (CH_2Cl_2/hexane, 70:30 v/v; $R_f = 0.45$) and crystallized from CH_2Cl_2/MeOH to provide **2** as a yellowish solid (246 mg, 29 %). ^{1}H NMR (400 MHz, $CDCl_3$): $\delta = 0.94$ (t, $J = 7.2$ Hz, 12H), 1.43 (m, 24H), 2.29 (m, 8H), 4.65 (d, $J = 7.9$ Hz, 4H), 4.95 (t, $J = 8$ Hz, 4H), 5.70 (d, $J = 7.9$ Hz, 4H), 6.57 (s, 4H), 6.78 (d d, $J = 7.5$ and 2 Hz, 8H), 7.26 (s, 4H), 7.36 (t, $J = 7.9$ Hz, 4H), 8.46 (s, 8H).

Ferrocene hemicarceplex with phenylethyl feet (Fc·**1**): To a solution of hemicarcerand **1** (23 mg, 0.011 mmol) in tripiperidinophosphine oxide (2 mL), ferrocene (200 mg, 1.07 mmol) was added. The reaction mixture was stirred for three days at 90 °C under a nitrogen atmosphere. The

  0947-6539/98/0405-0865 $ 17.50+.25/0

solution was cooled to room temperature and the product was chromatographed on silica gel (CH_2Cl_2/hexane, 70:30 v/v; $R_f = 0.40$) and crystallized from CH_2Cl_2/MeOH to provide Fc·**1** as a yellowish solid. ^{1}H NMR (400 MHz, $CDCl_3$): $\delta = 2.6-2.8$ (m, 16H), 3.81 (s, 10H), 4.63 (d, $J = 7.4$ Hz, 4H), 5.11 (t, $J = 8$ Hz, 4H), 5.93 (d, $J = 7.7$ Hz, 4H), 7.0 (d d, $J = 7.9$ and 2 Hz, 8H), 7.28 (m, 20H),7.35 (s, 4H), 7.36 (s, 4H), 7.58 (t, $J = 7.7$ Hz, 4H), 8.65 (s, 8H).

Ferrocene hemicarceplex with pentyl feet (Fc·**2**): To a solution of hemicarcerand **2** (23 mg, 0.011 mmol) in tripiperidinophosphine oxide (2 mL), ferrocene (200 mg, 1.07 mmol) was added. The reaction mixture was stirred for three days at 90 °C under a nitrogen atmosphere. The solution was cooled to room temperature and the product was chromatographed on silica gel (CH_2Cl_2/hexane, 70:30 v/v; $R_f = 0.45$) and crystallized from CH_2Cl_2/MeOH to provide Fc·**2** as a yellowish solid. FAB-MS (3-nitrobenzyl alcohol): 2332.3 [M^+], 2148.2 [$M^+ -$ Fc]. ^{1}H NMR (400 MHz, $CDCl_3$): $\delta = 0.93$ (t, $J = 7.4$ Hz, 12H), 1.4 (m, 24H), 2.23 (m, 8H), 3.66 (s, 10H), 4.48 (d, $J = 7.4$ Hz, 4H), 4.87 (t, $J = 8$ Hz, 4H), 5.79 (d, $J = 7.4$ Hz, 4H), 6.85 (d d, $J = 7.7$ and 2 Hz, 8H), 7.13 (s, 4H), 7.18 (s, 4H), 7.44 (t, $J =$ 8 Hz, 4H), 8.51 (s, 8H).

Equipment:^{1}H NMR spectra were obtained with a 400 MHz Varian VXR-400 spectrometer. Mass spectra were recorded at the University of Illinois Mass Spectroscopy Facility. Electrochemical experiments were performed with a Bioanalytical Systems 100B/W workstation equipped with a low-current module and controlled by a 100 MHz Pentium-based Gateway personal computer. The Digi-Sim 2.1 software[24] for the digital simulation work was run on the same computer.

Procedures: The voltammetric experiments were performed with a small-volume cell (3.0 mL; Cypress Systems, Lawrence (KS)), equipped with a glassy-carbon working electrode (0.0078 cm^2), a platinum counter electrode, and an Ag/AgCl reference electrode. Ultramicroelectrode experiments were performed with a BAS carbon-fiber electrode (3.9 μm radius). Dichloromethane and tetrachloroethane (both HPLC grade) were handled under an inert atmosphere and transferred to the cell immediately before use. The solutions were deoxygenated and kept under an inert N_2 atmosphere throughout the electrochemical experiments. All experiments were performed at room temperature. The glassy-carbon working electrode was polished with 0.05-μm alumina on a felt surface before each voltammogram was recorded. The apparent standard rate constant for heterogeneous electron transfer (k^0) of the ferrocene guest was estimated by Nicholson's method.[25] The values obtained in this way were utilized in fitting digital simulations to the experimental voltammograms. From the optimization of the fittings, we obtained the charge-transfer coefficient (α) and diffusion coefficient (D_0) associated with the heterogeneous electron-transfer processes. The voltammograms obtained with ultramicroelectrode working electrodes were analyzed by the method of Mirkin and Bard.[26] Bulk electrolyses were carried out with a two-compartment glass cell using a Pt-mesh working electrode.

Results

Synthesis: Scheme 1 shows the final synthetic steps used for the preparation of the hemicarcerand hosts. The tetrabromo cavitands **3** and **4**, which were prepared according to published methods,[22, 23] were converted to the tetralithium analogues with *sec*-butyllithium in THF; their reaction with *N*-formylmorpholine produced the tetraaldehydes **5** and **6** after acidification with HCl. Hemicarcerands **1** and **2** were prepared by reaction of two equivalents of the tetraaldehyde with four equivalents of 1,3-diaminobenzene in CH_2Cl_2 under high-dilution conditions. The ferrocene hemicarceplexes were prepared by heating a mixture of the corresponding hemicarcerand host with a large excess of ferrocene in tripiperidinophosphine oxide for several days.[14]

Electrochemistry: The ferrocene (Fc) complex of **1** was found to be extremely insoluble in most solvents commonly used for

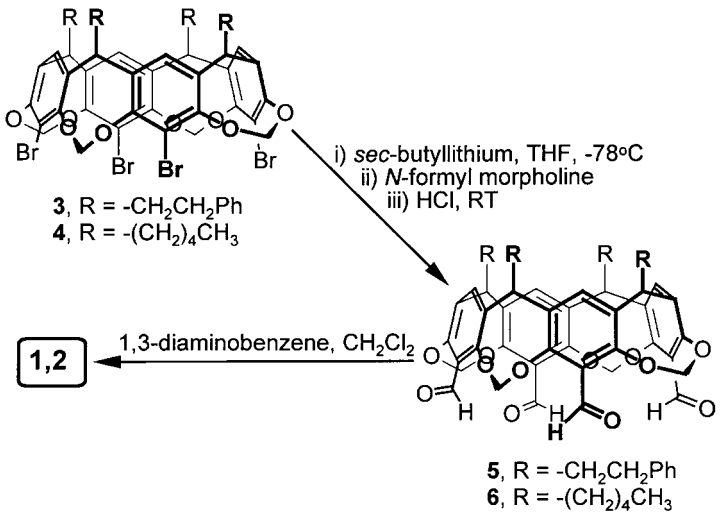

Scheme 1. Synthesis of hemicarcerands **1** and **2**.

electrochemical experimentation. Its electrochemical behavior could only be investigated in tetrachloroethane ($C_2H_2Cl_4$). Hemicarceplex Fc·**2** was sufficiently soluble in both dichloromethane and tetrachloroethane. Guest release from Fc·**2** in CD_2Cl_2 and Fc·**1** and Fc·**2** in $C_2D_2Cl_4$ at 25 °C was monitored by ^{1}H NMR spectroscopy. The half-life for these processes was found to be quite long ($t_{1/2} > 300$ h in all cases) which is consistent with Cram's reported value[14] of $t_{1/2} = 19.6$ h obtained with Fc·**1** at a much higher temperature (112 °C in $C_2D_2Cl_4$). These data clearly indicate that the kinetic stability of the two ferrocene hemicarceplexes is sufficient to provide a convenient time window in which the electrochemical behavior of the fully encapsulated ferrocene guest can be investigated.

A typical set of voltammograms for Fc·**2** in 0.15 M tetrabutylammonium hexafluorophosphate ($TBA^+PF_6^-$)/CH_2Cl_2 is shown (A in Figure 2). The observed voltammetric

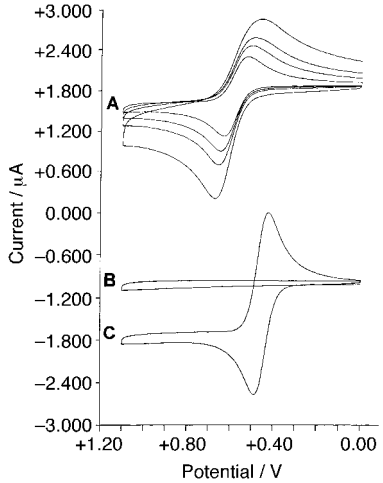

Figure 2. A)Cyclic voltammetric response on a glassy-carbon electrode (0.0078 cm^2) of a 1.0 mM solution of Fc·**2** in CH_2Cl_2/0.15 M $TBA^+PF_6^-$. Scan rates: 0.100, 0.175, 0.250, and 0.500 $V s^{-1}$. B) Cyclic voltammetric responses on the same electrode of a 1.0 mM solution of **2** (scan rate: 0.100 $V s^{-1}$) and C) of a 1.0 mM solution of Fc (scan rate: 0.100 $V s^{-1}$) in CH_2Cl_2/0.15 M $TBA^+PF_6^-$.

0947-6539/98/0405-0866 $ 17.50+.50/0 *Chem. Eur. J.* **1998**, *4*, No. 5

waves correspond to the monoelectronic oxidation of the ferrocene guest, as demonstrated by their absence in control voltammograms recorded with the uncomplexed hemicarcerand host (Figure 1, trace B). The half-wave potential for the encapsulated redox couple ($E_{1/2} = +0.57$ V versus Ag/AgCl) is considerably more positive than that observed for free ferrocene in the same medium ($E_{1/2} = +0.45$ V versus Ag/AgCl), indicating that the oxidized (cationic) form of the guest is relatively destabilized inside the rather nonpolar solvation shell provided by host **2**. In addition to this, the potential difference between the anodic and cathodic peak potentials (ΔE_p) was found to be larger than the theoretical value[27] expected for a reversible redox couple at the scan rates surveyed ($\nu > 50\,\mathrm{mV\,s^{-1}}$), demonstrating quasi-reversible kinetics of ET between Fc·**2** and the electrode surface.[28] Similar results were obtained for the two hemicarceplexes in $C_2H_2Cl_4$ solutions (see Figure 3). We recorded the ΔE_p values

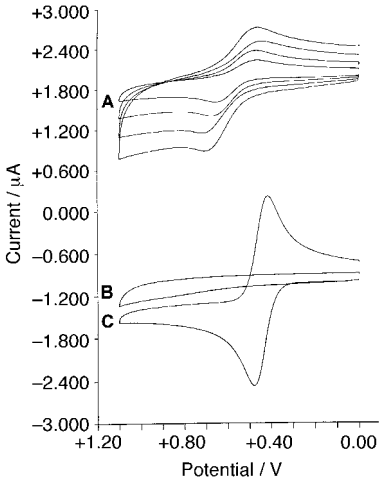

Figure 3. A) Cyclic voltammetric response on a glassy-carbon electrode (0.0078 cm^2) of a 1.5 mM solution of Fc·**1** in $C_2H_2Cl_4$/0.15 M $TBA^+PF_6^-$. Scan rates: 0.100, 0.250, 0.500, and 0.750 $V\,s^{-1}$. B) Cyclic voltammetric responses on the same electrode of a 1.0 mM solution of **1** (scan rate: 0.100 $V\,s^{-1}$) and C) of a 1.0 mM solution of Fc (scan rate: 0.100 $V\,s^{-1}$) in $C_2H_2Cl_4$/0.15 M $TBA^+PF_6^-$.

as a function of scan rate, and estimated the apparent standard rate constant for heterogeneous electron transfer (k^0) by Nicholson's method. These values were further used in digital simulations from which we obtained the corresponding charge-transfer coefficients (α) and diffusion coefficients (D_0). A summary of all the electrochemical data obtained is given in Table 1.

Table 1. Electrochemical parameters (obtained using conventional size working electrodes) for free ferrocene and ferrocene hemicarceplexes at 25°C in the indicated solvent containing 0.15 M $TBAPF_6$.

Compound	Solvent	$E_{1/2}$(V vs Ag/AgCl)	α	k^o[$cm\,s^{-1}$]	D_o [$cm^2\,s^{-1}$]
Fc	CH_2Cl_2	0.45	0.53	0.043	3.1×10^{-5}
Fc·**2**	CH_2Cl_2	0.57	0.31	0.0041	1.3×10^{-6}
Fc	$C_2H_2Cl_4$	0.46	0.55	0.0036	6.0×10^{-6}
Fc·**1**	$C_2H_2Cl_4$	0.56	0.39	0.00016	2.2×10^{-7}
Fc·**2**	$C_2H_2Cl_4$	0.54	0.43	0.00037	6.7×10^{-7}

Several clear trends emerge from the data given in Table 1. First, the half-wave potential for ferrocene oxidation is substantially more positive inside each hemicarcerand host than for uncomplexed ferrocene in the two solvents investigated. Second, encapsulation lowers the apparent standard rate constant for heterogeneous electron transfer by a factor of at least 10. This kinetic effect is also observed in each solvent medium. In $C_2H_2Cl_4$, where the two hemicarceplexes Fc·**1** and Fc·**2** can be directly compared, the phenylethyl hemicarcerand (host **1**) seems to depress the k^0 value more than the pentyl hemicarcerand (host **2**). The same order also holds for the expected decrease in the diffusion coefficient observed upon encapsulation in either host. The nature of the solvent markedly affects the k^0 and D_0 values observed for both uncomplexed and complexed ferrocene species. No changes were detected in the voltammetric behavior when the concentration of ferrocene hemicarceplex was varied in the range 0.5–2.0 mM, revealing that hemicarceplex aggregation does not play a significant role in the observed voltammetric behavior.

As there are problems associated with the use of Nicholson's method for the accurate determination of k^0 values, we performed a number of additional voltammetric experiments with ultramicroelectrodes. A comparison of the current–potential traces obtained with free Fc and Fc·**2** is shown in Figure 4. Qualitatively, these voltammograms reinforce the

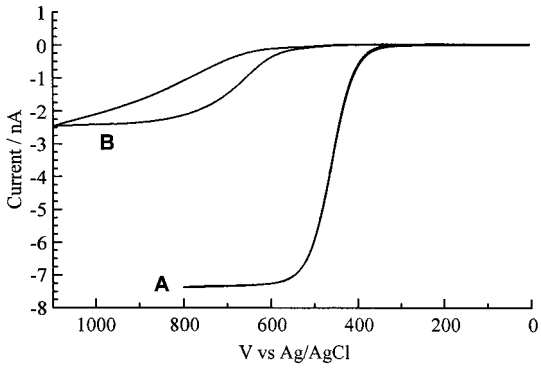

Figure 4. Voltammetric response on a carbon ultramicroelectrode of A) a 2.0 mM solution of Fc (scan rate: 10 $mV\,s^{-1}$) in CH_2Cl_2/0.15 M $TBA^+PF_6^-$ and B) a 4.0 mM solution of Fc·**2** (scan rate: 5 $mV\,s^{-1}$) in CH_2Cl_2/0.15 M $TBA^+PF_6^-$.

findings obtained with electrodes of conventional size. Hemicarcerand encapsulation leads to a more positive half-wave potential for the one-electron oxidation of ferrocene, a substantially lower apparent diffusion coefficient, and slower kinetics of heterogeneous electron transfer. We obtained clear evidence for the last of these effects from the current–potential waves, which we analysed by the method of Mirkin and Bard. The corresponding electrochemical parameters obtained from ultramicroelectrode experiments are given in Table 2.

What is the kinetic stability of the oxidized hemicarceplexes? This is a crucial question. The electrochemical oxidation of the ferrocene guest yields a charged species, ferrocenium (Fc^+), which is expected to be poorly solvated inside the nonpolar hemicarcerand cavity. The lack of stability associ-

Table 2. Electrochemical parameters (obtained by using ultramicroelectrodes) for free Fc and hemicarceplex Fc·**2** in CH_2Cl_2/0.15 M $TBAPF_6$ at 25 °C.

Compound	$E_{1/2}$(V vs Ag/AgCl)	α	k^o[cm s^{-1}]	D_o [cm^2 s^{-1}]
Fc	0.45	0.43	0.33	2.5×10^{-5}
Fc·**2**	0.57	0.43	0.0071	4.0×10^{-6}

ated with inefficient solvation might result in faster release of the oxidized guest from the host cavity into the solution medium. We investigated this possibility by performing bulk electrolysis of Fc·**2** in dichloromethane. The anodic oxidation (at 0.82 V versus Ag/AgCl) of 9.0 mg of this hemicarceplex dissolved in 5.0 mL of $TBA^+PF_6^-/CH_2Cl_2$ solution proceeded smoothly and yielded a greenish–blue solution. The electrolysis was stopped after about 1.5 h, when the total anodic charge consumed was equivalent to 1.05 electrons per molecule of Fc·**2**. Figure 5 shows the cyclic voltammograms

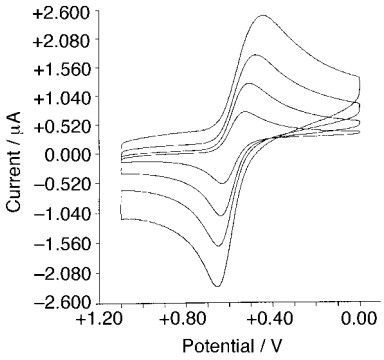

Figure 5. Cyclic voltammetric response on a glassy-carbon electrode (0.0078 cm^2) of a 1.0 mM solution of Fc·**2** in $C_2H_2Cl_4$/0.15 M $TBA^+PF_6^-$ after electrolysis (1.05 electrons per molecule) at +0.82 V vs. Ag/AgCl. Scan rates: 0.100, 0.250, 0.500, and 1.00 V s^{-1}.

recorded (initial potential = 1.1 V versus Ag/AgCl, negative forward scan) with the electrolyzed solution. The positions and shapes of the waves correspond very well with those observed before the bulk electrolysis. The half-wave potential for the only redox couple detected was 0.58 V versus Ag/AgCl, which is identical within the margin of error to that previously obtained for the $Fc^+ \cdot$ **2**/Fc·**2** redox couple (see Table 1). Therefore these results clearly indicate that, upon oxidation, ferrocene remains inside the hemicarcerand not only during the time scale of the voltammetric experiments but also during the much longer duration of the bulk electrolysis. To verify this point further, methanol was added to the electrolyzed $Fc^+ \cdot$ **2**/$TBA^+PF_6^-/CH_2Cl_2$ solution, resulting in the precipitation of a blue solid. This solid must be the hexafluorophosphate salt of the oxidized form of the hemicarceplex ($Fc^+ \cdot$ **2**) since we confirmed in control experiments that methanol does not precipitate ferrocenium hexafluorophosphate from its $TBA^+PF_6^-/CH_2Cl_2$ solutions. The isolated precipitate was collected by filtration, dried, and analyzed by NMR spectroscopy. The ^{1}H NMR spectrum of the blue solid is shown in Figure 6 as trace D. The proton resonances of the oxidized sample are shifted and broadened compared with those observed in the spectra of free Fc and Fc·**2**. As shown in

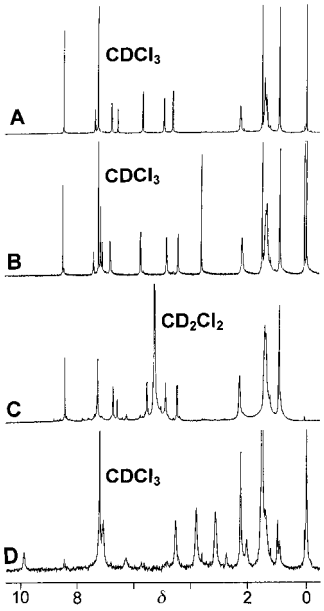

Figure 6. 400 MHz ^{1}H NMR spectra of A) **2** in $CDCl_3$, B) Fc·**2** in $CDCl_3$, C) an equimolar mixture of **2** and $Fc^+ \cdot PF_6^-$ in CD_2Cl_2, and D) a sample of $Fc^+ \cdot$ **2** in $CDCl_3$, prepared as described in the text.

Figure 6, the ^{1}H NMR spectrum of the oxidized sample is completely different from that obtained upon addition of one equivalent of ferrocenium hexafluorophosphate to a solution of uncomplexed hemicarcerand **2** (trace C). Spectrum D in Figure 6 is indeed consistent with the presence of a paramagnetic center (Fc^+) in the central cavity of **2** and further confirms the identity of the isolated solid as a salt of $Fc^+ \cdot$ **2**. The spectrum of this sample was monitored for several days to assess the guest release rate. However, the only spectral changes observed reveal the slow conversion of $Fc^+ \cdot$ **2** to Fc·**2**. No sign of faster release of the oxidized ferrocenium guest (compared with the ferrocene release rate) was detected.

Discussion

The selection of ferrocene as the electro-active guest for these experiments was dictated by synthetic concerns. The preparation of a ferrocene hemicarceplex with host **1** by Quan and Cram[14] played a crucial role in our decision to explore the electrochemistry of these systems. Ferrocene has frequently been used as a redox-active building block in the preparation of a variety of supramolecular assemblies[29] and is attractive from the electrochemical standpoint because it has a well-characterized and reversible anodic electrochemistry. However, Rusling and co-workers[30] have shown recently that the oxidation of ferrocene in acetonitrile (at Pt electrodes) yields insoluble films. Another potential complication related to the use of ferrocene as a guest results from the fact that the reported k^0 values for ferrocene cover a rather wide range and seem to correlate, at least partially, with electrode size.[28] This trend is evident in our own data, as we obtained a faster k^0 value for free ferrocene with ultramicroelectrodes; this is probably a reflection of imperfect compensation for ohmic drop in the measurements with electrodes of conventional

0947-6539/98/0405-0868 $ 17.50+.50/0 *Chem. Eur. J.* **1998**, *4*, No. 5

size. Therefore, we measured the apparent k^0 values for free ferrocene under the conditions of our experiments to validate the comparison with the values obtained for the encapsulated ferrocene species. Furthermore, under our voltammetric conditions we did not detect any film formation with either free or encapsulated ferrocene species.

Our electrochemical results demonstrate that ferrocene incarcerated by hemicarcerand hosts can readily engage in heterogeneous electron-transfer reactions. Molecular encapsulation does not necessarily render a redox center electroinactive. However, the electron-transfer processes are both thermodynamically and kinetically hindered compared with the corresponding processes involving the free, uncomplexed ferrocene. The thermodynamic hindrance is clearly demonstrated by the anodic shift observed in the half-wave potential for ferrocene oxidation upon encapsulation. This hindrance is probably related to the general difficulty associated with the generation of charges inside the nonpolar cavities of hemicarcerands. Cram and co-workers have detected large changes in the pK_a values of encapsulated molecules[16] that reflect the lack of adequate solvation of charged species inside these hosts.

Encapsulation also slows down the kinetics of the surveyed heterogeneous ET reactions. We observed at least a 10-fold decrease in the apparent k^0 values upon encapsulation. The reasons for this decrease must be related to the structural changes brought about by ferrocene encapsulation. According to current theory,[1–6] the standard rate constant for outer-sphere ET reactions is given by Equation (1), where k_e is the

$$k^0 = k_e A \exp(-\Delta G^{\neq}/RT) \quad (1)$$

electronic transmission coefficient (equal to unity for adiabatic reactions), A is the nuclear frequency factor, and $\Delta G^{\neq}$ is the activation free energy. The frequency factor A is expected to decrease linearly with $(m)^{1/2}$, where m is the molecular mass of the reactant.[4] Therefore, the ratio of the molecular masses of ferrocene and a ferrocene hemicarceplex may account for a factor of up to 3.5 in the observed decrease of the ET rate.[31] The degree of electronic coupling between the ferrocene center and the electrode surface is also affected by the distance over which the ET event must take place. Encapsulation inside the hemicarcerand markedly increases this distance. Using molecular modeling methods[32] we estimate that the minimum possible distance between the geometric center of the ferrocene nucleus and the electrode surface increases from about 3.5 to about 9 Å upon inclusion complexation by **1** or **2** (see Figure 7). However, our results were obtained with a very limited number of systems; additional experimental results with related systems are needed for the quantitative estimation of distance effects on ET rates.

The activation free energy ($\Delta G^{\neq}$) is composed of two terms. The first refers to the inner reorganization energy of the reactant. For ferrocene, this term is exceedingly small as the structural changes accompanying the ET process in uncomplexed ferrocene are minimal.[33] The second term is concerned with solvent reorganization, and important differences between free and hemicarcerand-encapsulated ferrocene may

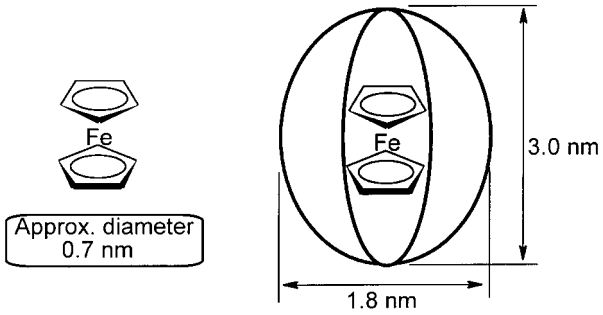

Figure 7. Comparison of approximate sizes of ferrocene and a

be expected here. A few years ago, Bard and co-workers reported that the rates of heterogeneous ET reactions are affected by solution viscosity,[34, 35] reflecting the involvement of solvent dynamics in the activation step. Many other reports have addressed the effects of solvent dynamics on the rates of outer-sphere ET reactions.[36–38] Similarly, the inside cavity walls of host **2** may act as an extremely rigid solvation shell or as a highly viscous solvent environment for the ferrocene center; this could account for a large fraction of the experimentally observed decrease in the ET rate constants upon encapsulation of the redox-active guest. Our data exhibit some clear solvent effects on the apparent k^0 values. For instance, the observed k^0 values for free ferrocene were lower in tetrachloroethane than in dichloromethane. This is perhaps a reflection of the slower solvent dynamics in the former solvent, which is expected from the relative molecular masses, but other factors (for instance, structure of the double layer) might be playing an important role. However, if the hemicarcerand were to act as a rigid solvation sphere, determining solvent reorganization effects and the heterogeneous ET rates in the hemicarceplexes, the kinetics for Fc·**2** would be expected to be essentially independent of the nature of the solvent. This expectation is not fulfilled experimentally, as the k^0 value for Fc·**2** was about an order of magnitude lower in tetrachloroethane than in dichloromethane. Therefore, our data do not support the idea that the solvent reorganization energy associated with ET processes in the hemicarceplexes is particularly high.

Balzani and co-workers[19] have measured the bimolecular rate constants for electron transfer quenching of the triplet state of free and encapsulated biacetyl by a variety of amines and other electron-donor quenchers, such as ferrocene itself. They found that the encapsulation of biacetyl by hemicarcerands decreased the ET quenching rate constant by a factor ranging from 10 to 10^4, depending on the nature of the quencher. Therefore, the effect of molecular encapsulation on the apparent k^0 values for ferrocene which was observed in our work is qualitatively consistent with the data reported by those authors. Furthermore, Farran et al. have investigated the isomerization of *cis*-piperylene sensitized by free and encapsulated acetophenone.[20] It may be inferred from their triplet energy transfer data that the hemicarcerand skeleton is involved in the simultaneous exchange of electrons between the HOMO and LUMO of the donor–acceptor pair. This suggests that the hemicarcerand aromatic structure may mediate the electronic coupling between the encapsulated

ferrocene center and the electrode surface, but further electrochemical experimentation with other hemicarceplexes is needed to verify this point.

Conclusions

From the results described here, we can conclude that the two main factors determining the slower heterogeneous ET rates in ferrocene hemicarceplexes than in free ferrocene are: i) the increase in the effective molecular mass of the electro-active species; and ii) the increased distance of maximum approach of the redox-active center to the electrode surface. The results presented in this work constitute the first measurements of heterogeneous ET reactions of fully encapsulated redox-active centers, but more data are necessary in order to evaluate fully the magnitude of the thermodynamic and kinetic effects brought about by constrictive molecular encapsulation. Our group is currently working on the preparation of other electro-active hemicarceplexes, using different redox-active guests and modified hemicarcerand hosts which may help to overcome the solubility limitations imposed by hosts **1** and **2**.

Acknowledgments: The support of this research by the NSF (CHE-9304262 and CHE-9633434 to A.E.K.) is gratefully acknowledged. We thank Marielle Gómez-Kaifer for help with several NMR experiments. We also acknowledge Professor D. J. Cram and his research group for the gift of a sample of hemicarcerand **1** at an early stage of this work.

Received: October 21, 1997 [F861]

[1] R. A. Marcus, *Angew. Chem.* **1993**, *105*, 1161; *Angew. Chem. Int. Ed. Engl.* **1993**, *32*, 1111.
[2] R. A. Marcus, N. Sutin, *Biochim. Biophys. Acta* **1985**, *811*, 265.
[3] N. Sutin, *Acc. Chem. Res.* **1982**, *15*, 275.
[4] R. A. Marcus, *J. Chem. Phys.* **1965**, *43*, 679.
[5] R. A. Marcus, *Annu. Rev. Phys. Chem.* **1964**, *15*, 155.
[6] N. S. Hush, *Faraday Trans.* **1961**, *57*, 557.
[7] For a recent comprehensive review, see: J. M. Lehn, *Supramolecular Chemistry*, VCH, Weinheim, **1995**.
[8] T. Matsue, D. H. Evans, T. Osa, N. Kobayashi, *J. Am. Chem. Soc.* **1985**, *107*, 3411.
[9] R. Isnin, C. Salam, A. E. Kaifer, *J. Org. Chem.* **1991**, *56*, 35.
[10] A. Mirzoian, A. E. Kaifer, *Chem. Eur. J.* **1997**, *3*, 1052.
[11] Y. Wang, S. Mendoza, A. E. Kaifer, *Inorg. Chem.* **1998**, *37*, 317.
[12] E. Córdova, R. A. Bissell, A. E. Kaifer, *J. Org. Chem.* **1995**, *60*, 1033.
[13] D. J. Cram, J. M. Cram, *Monographs in Supramolecular Chemistry*, *Vol. 4: Container Molecules and Their Guests* (Ed.: J. F. Stoddart), Royal Society of Chemistry, Cambridge, **1994**, ch. 8–10.
[14] M. L. C. Quan, D. J. Cram, *J. Am. Chem. Soc.* **1991**, *113*, 2754.
[15] D. J. Cram, M. E. Tanner, R. Thomas, *Angew. Chem. Int. Ed. Engl.* **1991**, *30*, 1024.
[16] D. J. Cram, M. E. Tanner, C. B. Knobler, *J. Am. Chem. Soc.* **1991**, *113*, 7717.
[17] T. A. Robbins, D. J. Cram, *J. Am. Chem. Soc.* **1993**, *115*, 12199.
[18] F. Pina, A. J. Parola, E. Ferreira, M. Maestri, N. Armaroli, R. Ballardini, V. Balzani, *J. Phys. Chem.* **1995**, *99*, 12701.
[19] A. J. Parola, F. Pina, E. Ferreira, M. Maestri, V. Balzani, *J. Am. Chem. Soc.* **1996**, *118*, 11610.
[20] A. Farran, K. D. Deshayes, C. Matthews, I. Balanescu, *J. Am. Chem. Soc.* **1995**, *117*, 9614.
[21] A. Farran, K. D. Deshayes, *J. Phys. Chem.* **1996**, *100*, 3305.
[22] J. A. Tucker, C. B. Knobler, K. N. Trueblood, D. J. Cram, *J. Am. Chem. Soc.* **1989**, *111*, 3688.
[23] J. A. Bryant, M. T. Blanda, M. Vincenti, D. J. Cram, *J. Am. Chem. Soc.* **1991**, *113*, 2167.
[24] M. Rudolph, D. P. Reddy, S. W. Feldberg, *Anal. Chem.* **1994**, *66*, 589A.
[25] R. S. Nicholson, *Anal. Chem.* **1965**, *37*, 1351.
[26] M. V. Mirkin, A. J. Bard, *Anal. Chem.* **1992**, *64*, 2293.
[27] A. J. Bard, L. R. Faulkner, *Electrochemical Methods: Principles and Applications*, Wiley, New York, **1980**, ch. 6.
[28] The small currents recorded in these voltammetric experiments (due to the small diffusion coefficient of the bulky Fc·**2** complex) guarantee that the ΔE_p values measured result from kinetic limitations and not from resistance effects.
[29] A. E. Kaifer, in: *Transition Metals in Supramolecular Chemistry*, (Eds.: L. Fabrizzi, A. Poggi), NATO ASI Series Kluwer, Dordrecht, **1994**, p. 227.
[30] G. N. Kamau, T. M. Saccucci, G. Gounili, A.-E. F. Nassar, J. F. Rusling, *Anal. Chem.* **1994**, *66*, 994.
[31] The molecular masses of Fc·**2** and Fc are 2332 and 186, respectively.
[32] These distances were estimated from both CPK models and molecular mechanics calculations (OPLS force field as implemented in the MACROMODEL software package).
[33] R. Martínez, A. Tiripicchio, *Acta Crystallogr. Sect. C* **1990**, *46*, 202.
[34] X. Zhang, J. Leddy, A. J. Bard, *J. Am. Chem. Soc.* **1985**, *107*, 3719.
[35] X. Zhang, H. Yang, A. J. Bard, *J. Am. Chem. Soc.* **1987**, *109*, 1916.
[36] H. Sumi, R. A. Marcus, *J. Chem. Phys.* **1986**, *84*, 4894.
[37] W. R. Fawcett, C. A. Foss, *J. Electroanal. Chem.* **1988**, *252*, 221.
[38] M. J. Weaver, *Chem Rev.* **1992**, *92*, 463.

  0947-6539/98/0405-0870 $ 17.50+.50/0